

PROTOCOL NOTE

Rapid imaging in the field followed by photogrammetry digitally captures the otherwise lost dimensions of plant specimens

Nicole James^{1,2} | Alex Adkinson^{1,2} | Austin Mast^{2,3} 

¹Department of Art, Florida State University, 540 West Call Street, Tallahassee 32301, Florida, USA

²Institute for Digital Information and Scientific Communication (iDigInfo), Florida State University, 142 Collegiate Loop, Tallahassee 32306, Florida, USA

³Department of Biological Science, Florida State University, 319 Stadium Drive, Tallahassee 32306, Florida, USA

Correspondence

Austin Mast, Department of Biological Science, Florida State University, 319 Stadium Drive, Tallahassee, Florida 32306, USA.
Email: amast@fsu.edu

This article is part of the special issue “Advances in Plant Imaging across Scales.”

Abstract

Premise: We recognized the need for a customized imaging protocol for plant specimens at the time of collection for the purpose of three-dimensional (3D) modeling, as well as the lack of a broadly applicable photogrammetry protocol that encompasses the heterogeneity of plant specimen geometries and the challenges introduced by processes such as wilting.

Methods and Results: We developed an equipment list and set of detailed protocols describing how to capture images of plant specimens in the field prior to their deformation (e.g., with pressing) and how to produce a 3D model from the image sets in Agisoft Metashape Professional.

Conclusions: The equipment list and protocols represent a foundation on which additional improvements can be made for specimen geometries outside of the range of the six types considered, and an easy entry into photogrammetry for those who have not previously used it.

KEYWORDS

Agisoft Metashape, biodiversity specimen collection, field work, herbarium, photogrammetry, photography, structure from motion (SfM), three-dimensional models

Resumen

Premisa: Reconocimos la necesidad de un protocolo de captura de imágenes adaptado a los requerimientos particulares de especímenes de plantas en el momento de la recolección, con el propósito de modelado 3D, así como la falta de un protocolo de fotogrametría de aplicación general que considere la heterogeneidad de las geometrías de especímenes de plantas y los desafíos introducidos por procesos como el marchitamiento.

Métodos y Resultados: Desarrollamos una lista de equipos y un conjunto de protocolos detallados (Módulos de Protocolo A–G) que describen cómo capturar imágenes de especímenes de plantas en el campo antes de su deformación (p. ej., al prensar) y cómo producir un modelo 3D a partir de un conjunto de imágenes utilizando Agisoft Metashape Professional.

Conclusiones: La lista de equipos y protocolos representan una base sobre la cual se pueden realizar mejoras adicionales para geometrías de especímenes fuera del rango de los seis tipos tomados en consideración, así como una introducción fácil a la fotogrametría para aquellos que no la han utilizado previamente.

This is an open access article under the terms of the Creative Commons Attribution-NonCommercial License, which permits use, distribution and reproduction in any medium, provided the original work is properly cited and is not used for commercial purposes.

© 2023 The Authors. *Applications in Plant Sciences* published by Wiley Periodicals LLC on behalf of Botanical Society of America.

The three-dimensional (3D) shape and size of organisms are important means by which humans have historically identified significant variation in the Earth's macroscopic biota, and factor into the many interactions between members of that biota and the biotic and abiotic features of their environment. Despite this, preservation of the shape and size of many organisms via specimen collection remains challenged by what can be a rapid distortion after death, sometimes hastened by collection methods (e.g., flattening of plant specimens in a press). Small numbers of two-dimensional (2D) images of organisms taken prior to collection can suggest shape and size but can be difficult to quantify accurately (e.g., for estimates of volume). The creation of digital 3D models of organisms in the field at the time of specimen collection has the potential to digitally preserve their shape and size for many later research uses, as well as to facilitate exciting education and outreach experiences in virtual and mixed reality settings.

Photogrammetry, especially via structure from motion (SfM), has emerged as a popular 3D modeling approach in the biodiversity sciences. Photogrammetry involves the inference of a 3D model from multiple images of a subject (Granshaw, 2016), and SfM algorithms rely on the identification of shared points of a subject in 2D images from multiple views (Brecko and Mathys, 2020; our references to “photogrammetry” throughout are references to photogrammetry via SfM). These 2D images can be taken with widely available commercial cameras (or those in mobile devices), rather than the dedicated equipment required for other 3D modeling approaches reviewed for natural history collections by Nieva de la Hidalgo et al. (2019) and Brecko and Mathys (2020). Because many cameras and their accessories have been designed to be mobile and for outdoor use, photogrammetry has been implemented widely in field conditions, providing insights into areas such as lichen colonization (Hincliffe et al., 2017), the size of Weddell seals (Beltran et al., 2018), coral growth rates (Lange and Perry, 2020), and many others. Measurements of models produced via photogrammetry can be comparable to those from the physical subject, as demonstrated for plants in agricultural research studies (e.g., Gao et al., 2021), and to those from other modeling approaches, as demonstrated for skeletons by Giacomini et al. (2019; compared with laser scanning and micro-computed tomography). Unlike some other 3D approaches (e.g., computed tomography and light detection and ranging [LiDAR]), photogrammetry can produce detailed, color-accurate surfaces for a 3D model. Brecko and Mathys (2020) calculated that photogrammetry is the most cost-effective way to produce 3D models in a natural history collection setting (as compared with laser scanning, structured light scanning, and computed tomography scanning when digitization involves up to 10,000 specimens).

Here, we introduce a detailed equipment list and set of eight protocol modules that can be combined in a workflow that researchers at any experience level can use to produce 3D models to document much of the heterogeneity seen in

plant collections intended to be archived on a herbarium sheet or in a carpological collection. The work fills a previous gap in digitization resources for plant collectors. Notably, the two extensive reviews of the potential for 3D modeling in natural history collections (Nieva de la Hidalgo et al., 2019; Brecko and Mathys, 2020) have between them only one brief reference to an approach for plants (Figure 16 in Nieva de la Hidalgo et al., 2019), and just 1% of the 3D models at MorphoSource (<https://www.morphosource.org/>; a site for sharing research-quality models) are plants, as of February 2023. Where plants have been the subject of 3D modeling in other contexts, especially in agricultural research, the focus is largely on high-throughput phenotyping, in which a workflow is optimized for a particular species (e.g., maize) or a particular part of a particular species (e.g., maize panicles) using heavily customized equipment (Gao et al., 2021). Some of that optimization involves alternative modeling methods (e.g., range imaging devices; Paulus et al., 2014), which can potentially address some of the known challenges for photogrammetry, such as the difficulty of rendering transparent structures, reflective surfaces, deep crevices, closely overlapping structures, and very thin structures, as well as the management and storage of the many (often large) image files produced. We experienced all these challenges in our work and attempt to address most of them in our protocol modules. With experience applying photogrammetry across the wide diversity of plant morphologies, we found it possible to predict which approaches will produce great 3D models (sometimes with additional workflow steps) and which might not, and we present our initial typology of plant morphologies in the context of likely photogrammetry success in a later section.

METHODS AND RESULTS

The equipment list (Appendix 1) describes the equipment used for image capture in the field (#1–32), and for image review, processing, and photogrammetry (#33–39). All items cited represent the equipment that we used over 18 months of experimentation (July 2021 to January 2023) while refining our approach. We present our methods in two sections below: (1) image capture and processing and (2) 3D modeling using photogrammetry. The methods are separated into eight protocol modules, two of which (A and B) are relevant to (1) and six of which (C–H) are relevant to (2).

Image capture and processing

The imaging activities are the part of the workflow that we designed to occur in the field, although photogrammetry can also start there, should you expect a subject to offer special challenges and you would like to get a sense of the adequacy of an imaging approach before leaving a field site.

Useful workflows are available for image capture indoors for photogrammetry (e.g., Brecko and Mathys, 2020; Medina et al., 2020; Gao et al., 2021), but we sought to produce a protocol that could be used by specimen collectors and others with a brief window of time to capture images before their subject's 3D geometry becomes distorted. We were guided by four considerations: (1) the method must be possible to deploy under field conditions, which can include bright sun, wind, rain, and the absence of a permanent power source; (2) the equipment should be multi-purpose so that it can be useful for additional activities beyond photogrammetry, which will help collectors justify the expenses; (3) the method should be fast, as field trips often involve short time periods; and (4) the method should accommodate subjects primarily in the size range of specimens collected for herbarium sheets (about 2.5–30 cm). The totality of the equipment involved probably limits the siting of a temporary field studio to within a short distance of the locations that you can reach in a vehicle (all-terrain or otherwise).

The goal in image capture for photogrammetry is to capture every outside surface of a subject with multiple images, each from a slightly different angle (angle shifted as little as 3–4°, as described by Medina et al. [2020], to 10°, as described by Brecko and Mathys [2020]). The camera can be rotated around the subject, as is the case for large, immobile subjects (e.g., with drone footage; Probst et al., 2018), or the subject can be rotated while the camera is stationary. In the latter option, the subject moves, but the relative positions of the subject's components to each other (e.g., the angle of the petals relative to the stem, as might be compromised when a flower wilts) should be maintained during imaging, if possible. This should be kept in mind if the subject is reoriented to make a new surface easier to capture. That is, if the subject changes its geometry in response to a new direction from which gravity is acting, it will not be possible to combine the image sets of the different subject orientations. If the subject is rotated and the cameras are stationary, as we do in Protocol Module A (Appendix S1), the scale bars should be a part of the scene that is rotating and appear in at least some of the images, although they do not need to be in any of the images from any one camera height. Scale bars can be captured from higher camera heights when the cameras are angled down, but they can be missed from low camera heights when the cameras are angled up.

The best models and textures will be achieved when every outer surface of a subject is not only present in multiple images but also in good focus in multiple images. Hence, it becomes important to understand what determines depth of field. The depth of field of an image is the range of the distance from the lens that is perceived to be in focus. Filling the field of view on our full-frame camera with our 50-mm macro lens and a subject that is 15 cm in height and 5 cm in depth produces distances from the lens to the edge of the subject that are about 30.5 cm. The depth of field for a particular camera, lens, aperture, and distance to the subject can be found using an online calculator (e.g., <https://www.dofmaster.com/dofjs.html>). In our case, with an f-stop

of $f/22$, we have a depth of field that is approximately 4.25 cm deep. If we open up our aperture to $f/16$ to let in more light, our depth of field is approximately 3 cm deep (1.25 cm less than for $f/22$). It is important to recognize that the distribution of the depth of field around your focal point is not necessarily half in front and half behind, although it is almost so in this scenario. Taking the f-stop from $f/16$ to $f/22$ reduces the size of the aperture by one-half, which leads to exposure (and diffraction) considerations.

Exposure is an important concept to understand in photography for photogrammetry. It is driven by three things that are adjusted in compensatory ways to produce good exposures: ISO, shutter speed, and aperture. A high ISO provides greater sensitivity to the light but produces images with more noise. A low ISO (e.g., 100) is generally recommended for photogrammetric software, although Medina et al. (2020) successfully used an ISO between 400–800 in their indoor studio. Permissible shutter speed is determined by the amount of movement of camera and subject. If the camera is mounted on a tripod, the wind blocked, and the subject settled to stationary after a turntable rotation and before the image is taken, we have found that we can use a shutter speed that is 1/10 second. This leads to acceptable exposures at $f/22$ that can be adjusted in Adobe Lightroom (Adobe, San Jose, California, USA) by +1.5 f-stops to produce good exposures for the images. Of the three variables affecting exposure, only aperture affects the depth of field. However, it can become important to keep in mind that when you are using small apertures (a large f-stop), diffraction of light can occur, which can introduce challenges to photogrammetry. Our camera body (Canon EOS 5D Mark IV; Canon, Tokyo, Japan) has a diffraction correction option, which we turn on at this higher f-stop, but this is only relevant to the in-camera corrections made to the JPG images. We correct diffraction in RAW (CR2) image files in Adobe Lightroom at the time of producing derivative images from them (TIFs).

Imaging a subject without supplemental light at $f/22$ can lead to severe underexposure, which can produce complications in photogrammetry. Our set-up produces substantial diffuse light using the LED lights of the Foldio (Orange-Monkie, San Diego, California, USA) set-up (with up to 4800 lumens, a color temperature of 5600 K, and a color rendering index at 95+; Figure 1) and a camera-mounted supplementary LED panel (up to 915 lumens at 5500 K of unknown color rendering index). The subject should not have strong shadows that change in their relative orientation to the subject's position (as would happen if the turntable was simply used in strong direct sun) unless those shadows are not part of the image (or are masked). We do not use a flash, although others do (e.g., Kano, 2022).

The Foldio turntable greatly speeds up image capture relative to the time that it would take to manually rotate a turntable and trigger shutter releases. It accomplishes this by way of an app that can program the turntable to stop 24, 36, or 48 times in a full rotation (corresponding to images offset by 15°, 10°, or 7.5°, respectively) and trigger a shutter



FIGURE 1 The battery-powered Foldio set-up with our two cameras on tripods set at different heights and a supplementary LED light on the hot shoe of the lower camera inside our pop-up work shelter. The scene demonstrates the use of an alligator clip to support the positioning of a branch in the center of the turntable, with the end of the branch anchored in a water-containing Eppendorf tube surrounded by modeling clay. The two 10-cm scale bars are attached to the turntable with double-sided tape.

release via infrared signal at each stop. We set up our two cameras on tripods at different heights (often about 76 cm [30 in] and 102 cm [40 in]) to capture different angles of view as the turntable makes each stop. These can then be set at new heights (for example, 89 cm [35 in] and 114 cm [45 in]) to capture two new angles of view as the turntable makes a second full rotation. With 48 turntable stops, we take 192 images of the subject in less than 5 min. If the subject orientation is flipped after the second rotation of the turntable for a third rotation, we can take 240 images of the subject in less than 8 min. We also capture an image of the ColorChecker Classic Mini (Calibrite, Wilmington, Delaware, USA) with each camera in each new lighting condition (in practice, once each day).

We did not explore focus stacking because speed was prioritized during image capture. Others have engineered imaging and rotation automation for focus stacking (e.g., Ströbel et al., 2018) in a studio setting, although this still takes considerably more time than our approach. The geometry of the subject determines the number of camera heights and stops on a full rotation that will be required for a good model and texture. Because the opportunity to capture the subject in 3D might be fleeting (e.g., if it is going to be flattened in a plant press), we recommend capturing images at 48 stops and four camera heights for every subject at the beginning. With experience you will get a sense for which subject geometries (e.g., a 5-cm-diameter subject like a round hickory fruit) can be reconstructed well with just two heights. The Foldio set-up does not work well with subjects greater than about 30 cm along the longest axis and 10 cm along the axis perpendicular to the longest axis, but this is also about the size limit for specimens that will fit on herbarium sheets.

The subject should be situated with the long axis extending vertically at the center point of the turntable to minimize the depths of the subject. Our strategy for supporting the subject in that orientation at that spot depends on the geometry and distribution of weight of the subject. We used three support strategies: (1) modeling clay, which could be molded around the base of the subject, was used for many smaller subjects, sometimes with a water-filled Eppendorf (Hamburg, Germany) tube embedded in it to keep a stem hydrated; (2) an alligator clip at the end of a piece of 13-cm copper wire (with black insulation) anchored in a heavy base, which could grasp a stem and could be used in combination with a water-filled Eppendorf tube in clay (Figure 1); or (3) a large galvanized bushing that served as a base for wider subjects. We spray-painted some of the items in the second and third strategy matte black.

We moved the images over to a 4-TB external hard drive on our laptop after each subject. This gave us an opportunity to check the quality of the images to determine whether it was necessary to capture another pair of camera heights to compensate for blurriness in a section of the subject, as well as to keep up with file management. We had the camera create a pair of images (JPG and RAW) with each shutter release and write them to both memory cards in the camera (a CompactFlash [CF] card and a Secure Digital [SD] card). We moved the images over to a constrained folder structure on the hard drive from the CF card each time, formatting the CF card in the camera before imaging each new subject. This simplified file management and left backup copies of the images on the SD card that could be deleted once it was clear that none of the images for the day had been corrupted or lost in the initial file transfer. We suggest a folder and file naming strategy. We also recommend that everyone unfamiliar with MorphoSource upload a model to this research resource soon after they begin to produce them to recognize all the relevant data that should be documented (some of it while in the field) for each model using the MorphoSource upload forms.

We processed the RAW images in Adobe Lightroom before using derivative TIF files in the photogrammetry steps. Processing included applying a camera color profile for each new lighting condition for each camera derived using the software ColorChecker Camera Calibration (X-Rite, Grand Rapids, Michigan, USA) based on the images of the ColorChecker Classic Mini, as well as adjusting exposure, removing chromatic aberration, enabling lens corrections, and other potential edits (e.g., enhancing contrast).

3D modeling using photogrammetry

The imaging protocol described above can be used to produce images for any photogrammetry software. For practical reasons, our photogrammetry protocol focuses on just one, Agisoft Metashape Professional (formerly Photoscan; Agisoft, St. Petersburg, Russia), a commercial option that is widely used and works on macOS, Windows, and

Linux, unlike some of the other commercial options that have narrower operating system requirements (e.g., Reality Capture). Metashape incorporates an intuitive interface (Medina et al., 2020), offers discounted educational pricing, and has been tested for accuracy in measurement data in a diversity of use cases (e.g., Omari et al., 2021). The speed of processing in Reality Capture is faster than in Metashape (Medina et al., 2020), although we have used our images with success in that software as well. Further comparison between photogrammetric software applications for plant specimens is warranted, such as was performed in the landscape-scale studies by Probst et al. (2018) and Pell et al. (2022), but it is outside the scope of our work here.

We recognized that the diversity of 3D geometries that we captured in our image sets fell into six categories (Figure 2), which were somewhat predictive of the complexity of workflow that would be required for a successful outcome (or lack thereof). The geometry of the external surfaces of a subject is reproduced in a model (the “mesh”) constructed of many (potentially millions of) polygons, referred to as “faces.” (Granshaw [2020] is a useful resource for photogrammetry terminology, but some terms used frequently in Metashape [e.g., “faces”] are not

described in that resource.) The mesh is covered with an image file (the “texture”) that represents the combination of many image parts from across the image set. Some of these subject types (see Appendix S1) were straightforward to process, while others required additional steps to produce a successful mesh and texture. One (type A) is unlikely to produce a successful outcome using our protocols due to the complexity of closely overlapping fine structures in the subject. Subject types B–F are reasonably likely to produce great models and textures.

Photogrammetric processing of the image sets is detailed in Protocol Modules C–H (Appendix S1). Protocol Module C is a basic protocol dealing with the major steps from image alignment to mesh and texture export, which might be all that is needed for specimen types D–F; however, the processing of those specimen types (as well as types B and C) might benefit from Protocol Module D, which focuses on producing masks for the images. A mask removes the superfluous parts of an image (i.e., those that are not part of the subject) from consideration in the image alignment and, potentially, other steps, which can filter out points that might otherwise lead to geometry in the mesh that is not derived from the subject (Koutsoudis et al., 2013).

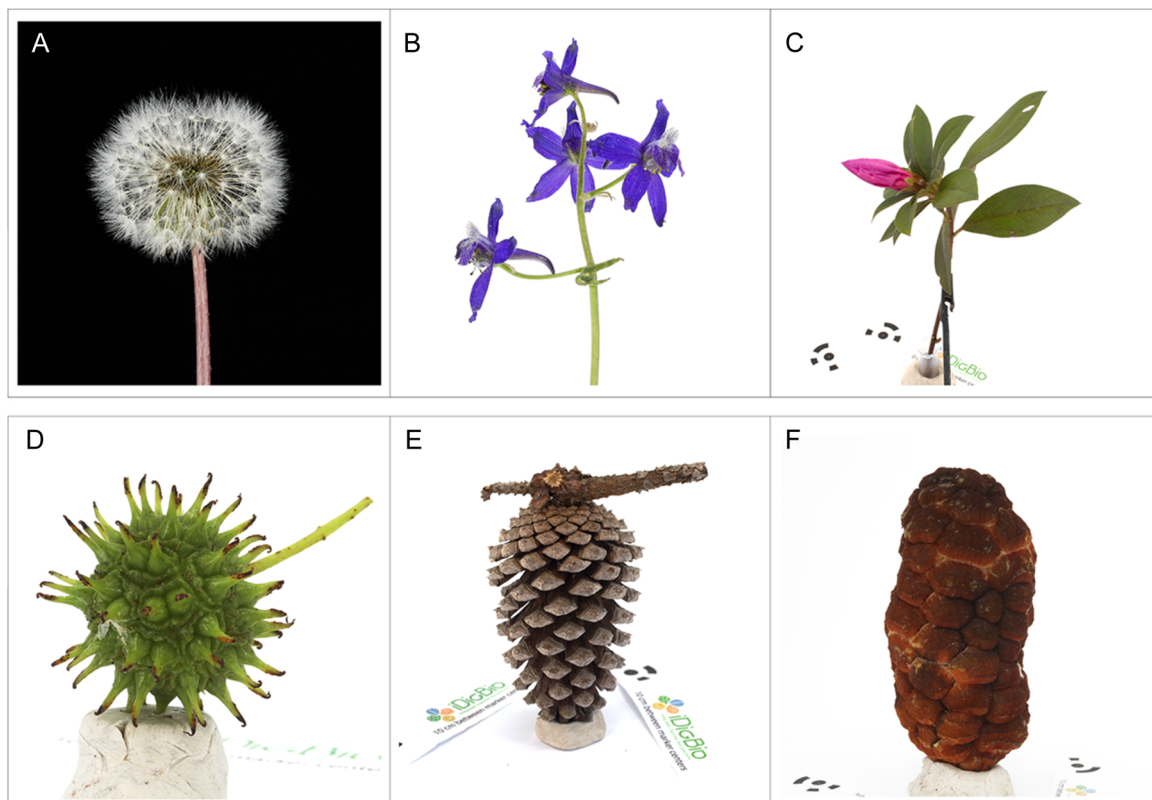


FIGURE 2 Illustration of our subject typology with links to the final models at Sketchfab for each. (A) High surface area:volume with thin features, commonly with close overlap of structures from every angle and thin features from every angle that is captured; did not produce viable model. (B) High surface area:volume with thin features only from some angles and a less close overlap of structures; model available at <https://skfb.ly/oDPA6>. (C) High surface area:volume with thicker features and little close overlap of structures; model available at <https://skfb.ly/oDPzL>. (D) Low surface area:volume with relatively few features that are thin from every angle, some overlap, and some crevices; model available at <https://skfb.ly/oDPzK>. (E) Low surface area:volume without thin features, but with some overlap and crevices; model available at <https://skfb.ly/oDPzS>. (F) Low surface area:volume without thin features, close overlap of features, or crevices; model available at <https://skfb.ly/oDPzI>.

Image alignment involves the recognition of points in the scene that are documented by multiple images (“tie points”). The positions of these tie points are inferred in a 3D space to produce a “sparse point cloud” after image alignment in Metashape; each point in the cloud is positioned relative to the cameras in a “depth map.” The visualization of the sparse point cloud and inferred camera positions serves as a major quality checkpoint. The sparse point cloud should approximate the appearance of the subject (and anchor and scale bars), and the inferred camera positions should appear as more or less parallel rings corresponding to the camera heights at which the images were captured (Figure 3). It is less straightforward to use inferred camera positions to check alignment quality when images are taken “free-hand” or with a manual turning of the turntable, which our protocol does not employ. If there is an apparent problem with either the point cloud or the inferred camera positions (or when we knowingly change the orientation of the subject relative to the turntable to image a previously obscured surface), we incorporate additional protocol modules. These modules deal

with image misalignments (Protocol Module E), managing and merging “chunks” (Protocol Module F), and mesh refinement (Protocol Module G).

Chunks are established to manage image sets and their derivatives (e.g., sparse point clouds) that document a single orientation or geometry of the subject. This could be a pine cone with the base down in one chunk and the pine cone with the base up in a second chunk (Figure 4). Alternatively, it could be the images of a sunflower upon first rotation of the turntable in one chunk and the images of the same sunflower in the same orientation in the second rotation of the turntable after the petals have slightly drooped in the second chunk. In both examples, we produce a point cloud from each chunk and then attempt to automatically (then manually, if needed) align and merge the chunks into a single point cloud describing the subject with which to then derive the mesh and texture.

When needed, we performed the manual alignment of chunks using dense point clouds. In the example documented in Figure 5, we noticed the first indication of a problem when we generated the mesh (Figure 5A), which

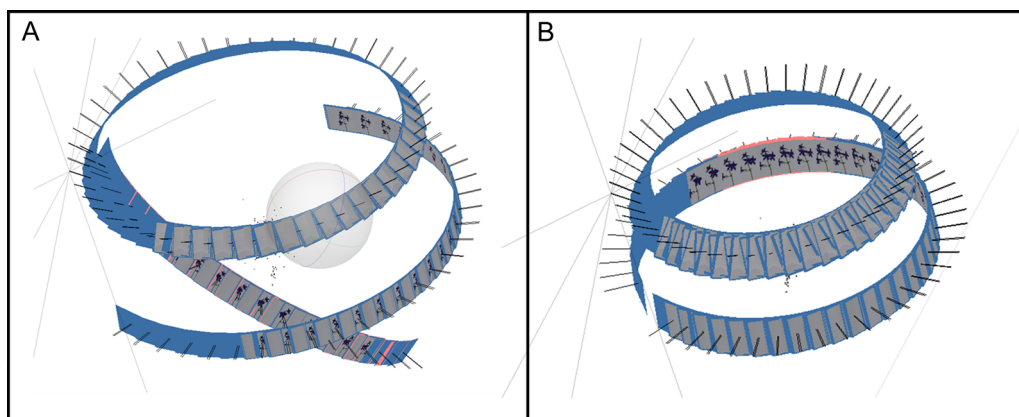


FIGURE 3 Incorrect vs. correct alignment of images, as determined by inferred camera position in Agisoft Metashape Professional. (A) The diagonal section of inferred camera positions indicates a misalignment given our turntable approach to imaging. (B) Proper alignment of images from two camera heights using our imaging protocol. The misaligned images in (A) were realigned to produce (B).

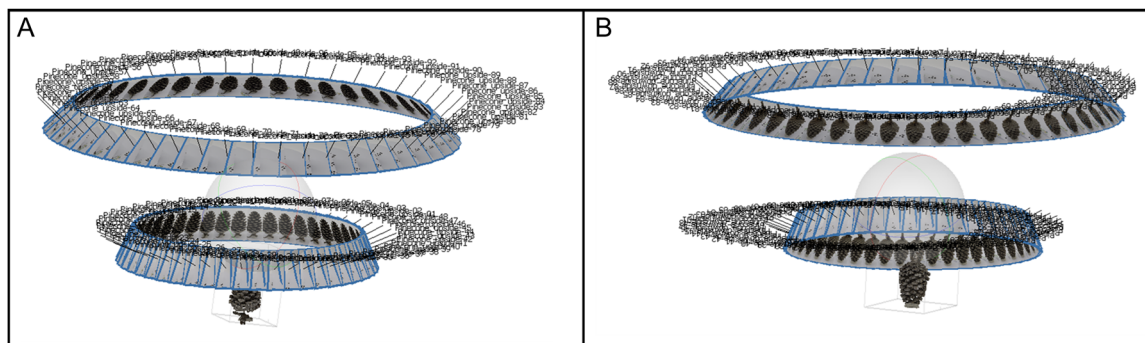


FIGURE 4 Example of separate alignments of images of different chunks in Agisoft Metashape Professional. (A) In Chunk 1, the pine cone is oriented with the base down. (B) In Chunk 2, the pine cone is oriented with the base up. These chunks could then be automatically aligned and merged, with the resultant depth maps used to produce a successful mesh.

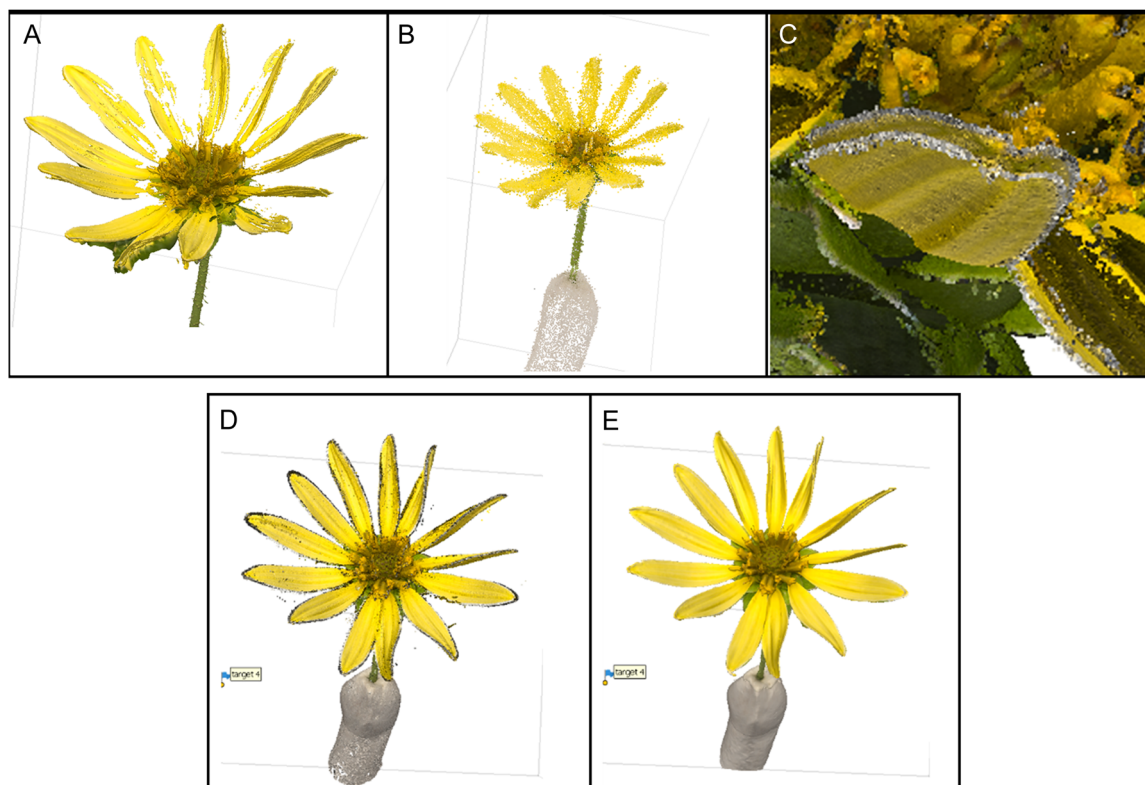


FIGURE 5 Managing the wilting of plants during image capture through the manual alignment of chunks in Agisoft Metashape Professional. (A) The mesh produced with all images in a single chunk. Holes appeared despite there not being holes in the sparse point cloud. (B) The sparse point cloud produced with all images in a single chunk. (C) Automatic alignment of sparse point clouds produced in two separate chunks. The two chunks corresponded to image sets produced during the two turntable rotations. (D) Further manual alignment of dense point clouds from (C). (E) The final textured mesh using the manual alignment of dense point clouds.

had holes in it that had not been present in the sparse point cloud (Figure 5B). We moved the images taken during the second rotation of the turntable into their own chunk and produced dense point clouds with each chunk. We then automatically aligned the chunks, which produced the duplication with slight offset of some petals (Figure 5C). We manually adjusted the alignment of the dense point cloud for one of those chunks to produce a better alignment (Figure 5D), which produced a good mesh and texture (Figure 5E). Note that manual adjustments of the alignment can compromise the model's value for morphometric study, but it also can produce models that are useful for other purposes, such as education or outreach.

We use dense point clouds for the manual alignment of chunks, but we do not use them in mesh creation as was done by some others (e.g., Brecko and Mathys, 2020). Instead, we use the depth map data produced during image alignment for mesh creation. In our experimentation, we found that meshes produced with the depth maps require less processing time and retain more of the subject's surface area than those produced via dense point clouds.

The appearance of the mesh serves as another quality checkpoint in the process, and we check it for missing geometry (e.g., the holes of Figure 5A) and inaccurate

roughness. These issues can be addressed using mesh smoothing and refinement (covered in Protocol Modules C and G, respectively). These issues can arise due to the reflectivity of the surface, as might be caused by moisture or morphological properties, such as in the example of Figure 6.

The mesh can be decimated to decrease the file size prior to export, which decreases the number of faces (e.g., from millions to 500,000). The target number of faces and final export formats will be dependent on the intended use for the model (e.g., in 3D printing or virtual reality scenes), as well as any requirements made by the website on which the model will be shared (e.g., MorphoSource or Sketchfab). Reducing the number of faces does not always lead to perceptible differences in the model's geometry (Agisoft Metashape, 2023). It is strategic to duplicate 3D models prior to decimation, keeping an original and (potentially) several size variations of it for different purposes. The mesh is then textured prior to export as one or more of various file types such as OBJ (the most common 3D file type), PLY (a potential improvement on OBJ because it is more extensible), STL (for 3D printing), and others. We found that PLY serves our purposes for uploading high-resolution meshes to MorphoSource, and discuss model export in greater depth in Protocol Module H.

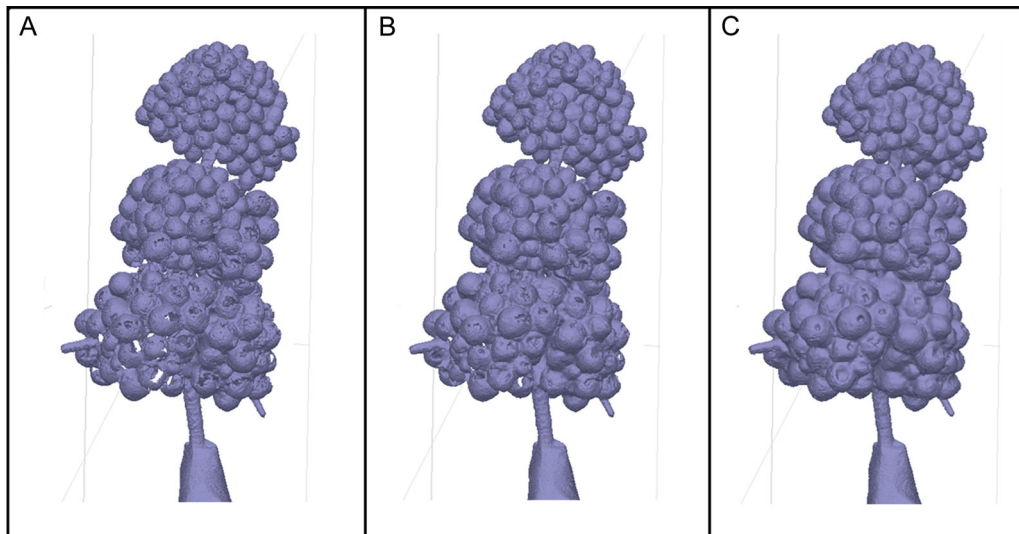


FIGURE 6 The impact of mesh refinement in Agisoft Metashape Professional. (A) The mesh produced with Protocol Module C without refinement with the quality set at ultra-high. Note the holes in the lower part of the subject where light reflection confounded the algorithm. (B) Mesh construction with refinement and quality set at high. Some holes remain. (C) Mesh construction with refinement with the quality set at medium. The mesh no longer contains the holes.

CONCLUSIONS

We intend our equipment list and protocol modules to provide a straightforward introduction to photogrammetry that can jump-start the 3D modeling of plants by collectors and form a foundation for future equipment and protocol extensions (e.g., that address new challenges in plant geometries). Our development of these resources was driven by our laser focus on considerations that should lead to compatibility with plant collector's activities, such as focusing on a size range typical of specimens mounted on herbarium sheets and the use of multi-purpose equipment. With this work, we seek to enable new possibilities for plant collectors to deliver added value with their specimens, perhaps leading to new collecting strategies (e.g., focused on describing the morphospace of flowers in a community), collaborations (e.g., with outreach professionals), training opportunities (e.g., in the emerging metaverse), and increased funding.

AUTHOR CONTRIBUTIONS

All three authors designed and refined the equipment list and protocol modules and wrote the paper. A.M. conceived of the project, secured funding, and supervised it. All authors approved the final version of the manuscript.

ACKNOWLEDGMENTS

We are grateful for helpful conversations with Zach Randall, Ed Stanley, David Blackburn, Nelson Rios, Joshua Medina, John McCormack, Duncan Irschick, Doug Boyer, and others; the helpful feedback from two anonymous reviewers; and assistance in the field and lab from Rick Williams at the Rocky Mountain Biological Laboratory. The Foldio set-up was first suggested to us by Eli Mast (Leon High School, Tallahassee,

Florida), although we later found a reference to it in an article by Brecko and Mathys (2020) as well. Fritz Pichardo-Marcano (Florida State University) translated the abstract into Spanish. The work represents gap-filling in biodiversity specimen digitization protocols by iDigBio, and Gil Nelson and David Jennings are gratefully acknowledged for their support. iDigBio is funded by grants from the National Science Foundation (DBI-1115210 [2011–2018], DBI-1547229 [2016–2022], and DBI-2027654 [2021–2026]). Any opinions, findings, and conclusions or recommendations expressed in this material are those of the author(s) and do not necessarily reflect the views of the National Science Foundation.

DATA AVAILABILITY STATEMENT

The meshes and image sets relevant to this project are available at Morphosource (<https://www.morphosource.org/projects/000494239?locale=en>). The data were uploaded and managed by Alex Adkinson.

ORCID

Austin Mast  <http://orcid.org/0000-0002-4995-0467>

REFERENCES

- Agisoft Metashape. 2023. Agisoft Metashape User Manual: Professional Edition, Version 2.0. Website: <https://www.agisoft.com/downloads/user-manuals/> [accessed 29 January 2023].
- Beltran, R. S., B. Ruscher-Hill, A. L. Kirkham, and J. M. Burns. 2018. An evaluation of three-dimensional photogrammetric and morphometric techniques for estimating volume and mass in Weddell seals *Leptonychotes weddellii*. *PLoS ONE* 13(1): e0189865. <https://doi.org/10.1371/journal.pone.0189865>
- Brecko, J., and A. Mathys. 2020. Handbook of best practice and standards for 2D+ and 3D imaging of natural history collections. *European Journal of Taxonomy* 623: 1–115. <https://doi.org/10.5852/ejt.2020.623>

- Gao, T., F. Zhu, P. Paul, J. Sandhu, H. A. Doku, J. Sun, Y. Pan, et al. 2021. Novel 3D imaging systems for high-throughput phenotyping of plants. *Remote Sensing* 13(11): 2113.
- Giacomini, G., D. Scaravelli, A. Herrel, A. Veneziano, D. Russo, R. P. Brown, C. Meloro, et al. 2019. 3D Photogrammetry of bat skulls: Perspectives for macro-evolutionary analyses. *Evolutionary Biology* 46: 249–259. <https://doi.org/10.1007/s11692-019-09478-6>
- Granshaw, S. I. 2016. Photogrammetric terminology: third edition. *Photogrammetric Record* 31: 210–252. <https://doi.org/10.1111/phor.12146>
- Granshaw, S. I. 2020. Photogrammetric terminology, fourth edition. *Photogrammetric Record* 35: 143–288. <https://doi.org/10.1111/phor.12314>
- Hinchliffe, G., B. Bolland-Breen, D. A. Cowan, A. Doshi, L. N. Gillman, G. Maggs-Kolling, A. de Los Rios, and S. B. Pointing. 2017. Advanced photogrammetry to assess lichen colonization in the hyper-arid Namib Desert. *Frontiers in Microbiology* 8: 2083. <https://www.frontiersin.org/articles/10.3389/fmicb.2017.02083>
- Kano, Y. 2022. Bio-photogrammetry: Digitally archiving coloured 3D morphology data of creatures and associated challenges. *Research Ideas and Outcomes* 8: e86985. <https://doi.org/10.3897/rrio.8.e86985>
- Koutsoudis, A., B. Vidmar, and F. Arnaoutoglou. 2013. Performance evaluation of a multi-image 3D reconstruction software on a low-feature artefact. *Journal of Archaeological Science* 40(12): 4450–4456. <https://doi.org/10.1016/j.jas.2013.07.007>
- Lange, I. D., and C. T. Perry. 2020. A quick, easy and non-invasive method to quantify coral growth rates using photogrammetry and 3D model comparisons. *Methods in Ecology and Evolution* 11: 714–726. <https://doi.org/10.1111/2041-210X.13388>
- Medina, J. J., J. M. Maley, S. Sannapareddy, N. N. Medina, C. M. Gilman, and J. E. McCormack. 2020. A rapid and cost-effective pipeline for digitization of museum specimens with 3D photogrammetry. *PLoS ONE* 15(8): e0236417. <https://doi.org/10.1371/journal.pone.0236417>
- Nieva de la Hidalga, A., P. Rosin, X. Sun, M. van Walsun, and Z. Wu. 2019. Rapid 3D capture methods in biological collections and related fields. Available at Zenodo repository: <https://doi.org/10.5281/zenodo.3469531> [posted 30 September 2019; accessed 15 December 2022].
- Omari, R., H. Cahill, J. Coumbaros, and B. Chapman. 2021. Virtual anthropology? Reliability of three-dimensional photogrammetry as a forensic anthropology measurement and documentation technique. *International Journal of Legal Medicine* 135: 939–950. <https://doi.org/10.1007/s00414-020-02473-z>
- Paulus, S., J. Behmann, A.-K. Mahlein, L. Plümer, and H. Kuhlmann. 2014. Low-cost 3D systems: Suitable tools for plant phenotyping. *Sensors* 14: 3001–3018. <https://doi.org/10.3390/s140203001>
- Pell, T., J. Y. Q. Li, and K. E. Joyce. 2022. Demystifying the differences between structure-from-motion software packages for pre-processing drone data. *Drones* 6(1): 24. <https://doi.org/10.3390/drones6010024>
- Probst, A., D. Gatzliolis, and N. Strigul. 2018. Intercomparison of photogrammetry software for three-dimensional vegetation modelling. *Royal Society Open Science* 5: 172192172192. <https://doi.org/10.1098/rsos.172192>
- Ströbel, B., S. Schmelzle, N. Bluethgen and M. Heethoff. 2018. An automated device for the digitisation and 3D modelling of insects combining extended-depth-of-field and all-side multi-view imaging. *ZooKeys* 759: 1–27. <https://doi.org/10.3897/zookeys.759.24584>

SUPPORTING INFORMATION

Additional supporting information can be found online in the Supporting Information section at the end of this article.

Appendix S1. This document outlines the detailed process for creating a 3D model from plant specimens collected in the field, from image capture to finalizing a model for export and upload.

How to cite this article: James, N., A. Adkinson, and A. Mast. 2023. Rapid imaging in the field followed by photogrammetry digitally captures the otherwise lost dimensions of plant specimens. *Applications in Plant Sciences* 11(5): e11547. <https://doi.org/10.1002/aps3.11547>

Appendix 1. Equipment list.

This list details equipment used for image capture in the field (#1–32) or for image review, processing, and photogrammetry (#33–39). All items cited represent the equipment that we used. All prices are provided in USD and are correct as of January 2023, when that information was available at the URL provided. Prices are listed without tax or shipping. Specifics are not given for generally available items (e.g., tape measure, pencil). Equipment was selected to be multi-purpose with more potential uses than photogrammetry alone, with the exception of the photogrammetry software.

1. **Pop-up work shelter with wind guards**, unless other shelters are available to protect the workspace from wind and rain and to diffuse full sunlight.
 - a. CLAM Quick-Set Venture Screen Tent (1; SKU 11287500, \$299.99; CLAM, Rogers, Minnesota, USA) <https://quicksetshelters.com/venture-screen-tent>
 - b. CLAM Quick-Set Wind and Sun Panel Attachment (1; SKU 9294-9896, \$34.99) <https://quicksetshelters.com/green-wind-panels>
2. **Portable battery and solar panel**, unless another power source is present (e.g., power outlet at a campsite). Solar panel is only necessary to recharge battery if it cannot be expected that the battery can be regularly recharged at a power outlet.
 - a. Jackery Solar Generator 1000, which is a bundling of Jackery Explorer 1000 + Jackery SolarSaga 100 W panel (1; \$1398.00; Jackery, Fremont, California, USA) <https://www.jackery.com/products/jackery-explorer-1000-2-x-solarsaga-100w-solar-generator>
3. **Lightbox and turntable**; a portable lightbox and app-controlled programmable turntable that can trigger shutter releases in the cameras with an infrared signal.
 - a. Foldio3 360 Studio Set, which is a bundling of the Foldio3 portable light box, Studio Backdrops (white and black), a Halo Bar (2), and a Foldio360 Smart Turntable (1; \$279; OrangeMonkie, San Diego, California, USA) <https://orangemonkie.com/products/foldio3?variant=40121548275851>
4. **Foldio360 App** (OrangeMonkie) on **smartphone or tablet** with a **charging cord** for the mobile device (free, if currently have smartphone or tablet).
 - a. <https://apps.apple.com/us/app/foldio360/id1144327537>

- b. https://play.google.com/store/apps/details?id=com.orangemonkie.foldio360&hl=en_US&gl=US
5. **DSLR or mirrorless camera bodies and manual(s).** We prefer two identical body types, although one could perform image capture with a single camera, with more than two cameras, or with cameras that are different models. Always keep the relevant manuals with you when using the camera(s) to address questions that arise.
 - a. Canon EOS 5D Mark IV DSLR Camera (2; SKU 1483C002, \$2499.00 each; Canon, Tokyo, Japan) (<https://www.usa.canon.com/shop/p/eos-5d-mark-iv?color=Black&type=New>)
 6. **Camera lenses.** We typically use identical lenses concurrently and have a pair of 50-mm macros and 100-mm macros on hand, adjusting the lenses on the cameras to the size of the subject (i.e., the two 50-mm macro lenses for larger subjects or the two 100-mm macro lenses for smaller subjects). We prefer prime (fixed focal length) lenses because they do not have the potential to inadvertently change the focal length during image capture (e.g., as might happen with a zoom lens that is positioned at an angle other than horizontal as gravity works on it).
 - a. EF 50 mm f/2.5 Compact Macro, or comparable lens (2; \$179.99 each; Canon) <https://www.amazon.com/Canon-50mm-Compact-Macro-Lens/dp/B00006153V>
 - b. EF 100 mm f/2.8 Macro USM, or comparable lens (2; \$349.00 each; Canon) <https://www.amazon.com/Canon-100mm-Macro-Fixed-Cameras/dp/B00004XOM3?th=1>
 7. **Memory cards** for image files (one for each slot type in each camera). Our camera bodies use CF and SF card types. The camera can be directed to write copies of each image file to both internal cards (which provides a backup copy should a card become corrupted) or write a single copy to one card until that card is full then switch to using the second card (which extends memory). Note: Many cheaper options exist for memory cards than the rugged versions that we use.
 - a. Sony 128 GB CFexpress Type B TOUGH Memory Card (2; \$219.99 each; Sony, Tokyo, Japan) https://www.bhphotovideo.com/c/product/1531996-REG/sony_cebg128_j_128gb_cfexpress_type_b.html
 - b. Sony 128 GB SF-G TOUGH Series UHS-II SDXC Memory Card (2; \$209.99 each) https://www.bhphotovideo.com/c/product/1437901-REG/sony_sf_g128t_t1_128gb_sf_g_series_tough.html
 8. **Camera batteries** (two per camera). The back-up battery for each camera can be charging while the other battery is in use, if needed.
 - a. Canon LP-E6NH Lithium-Ion Battery (4; \$79.00 each, and a battery is typically bundled with the camera body at time of purchase) https://www.bhphotovideo.com/c/product/1573782-REG/canon_lp_e6nh_lithium_ion_battery.html?fromDisList=y
 9. **Camera battery chargers** (one per camera)
 - a. Canon LC-E6, Model DS510101 (2; \$59.95 each, although a charger is typically bundled with the camera body at time of purchase) https://www.bhphotovideo.com/c/product/590433-REG/Canon_3348B001_LC_E6_Battery_Charger.html
 10. **LED light** to mount on the camera. This augments light from the lightbox. We originally had two of these, but one broke after a few months. There might be better alternatives to the Explorer product given below.
 - a. Explorer Photo and Video AuraLED 915 Bicolor LED On-Camera Light (1; \$69.95; Explorer Photo and Video, Los Angeles, California, USA) https://www.bhphotovideo.com/c/product/1630330-REG/explorer_photo_video_ax_led915_auraled_915_photography_fill.html
 11. **Tripods** (one per camera). The tripods should reach a height of at least 140 cm if your lightbox is sitting on a surface that is about 76 cm above the ground.
 - a. Manfrotto Befree Advanced Travel Aluminum Tripod with 494 Ball Head (2; \$199.95 each; Manfrotto, Cassola, Italy) https://www.bhphotovideo.com/c/product/1367494-REG/manfrotto_mkbfria4bk_bhush_befree_advanced_travel_tripod.html
 12. **Rugged camera equipment case**
 - a. Pelican 1560SC Studio Case (1; \$429.95; Pelican Products, Torrance, California, USA) https://www.bhphotovideo.com/c/product/1436921-REG/pelican_015600_0070_110_1560sc_protector_studio_case.html
 13. **Calibrite ColorChecker Classic Mini**
 - a. ColorChecker Classic Mini (1; \$69.00; Calibrite, Wilmington, Delaware, USA) <https://calibrite.com/us/product/colorchecker-classic-mini/>
 14. **Scale bars.** These can be created using the markers supplied online for Agisoft Metashape (Agisoft, St. Petersburg, Russia). We created two scale bars of different sizes using Agisoft's Circular 12-bit targets. A pair of 10-cm scale bars were taped onto the turntable using double-sided tape for larger subjects, while a smaller version (4-cm scale bar) is suspended with an alligator clip for smaller subjects that are captured with the 100-mm lenses.
 - a. <https://agisoft.freshdesk.com/support/solutions/articles/31000148855-coded-targets-and-scale-bars#How-to-Print-Coded-Targets>
 15. **Microfiber lens cleaning cloth and alcohol wipes** (or lens wipes)
 16. **Folding tables.** We use two tables (1.2 m long, ca. 76 cm high) if there are no available work surfaces at table height.
 17. **Folding chair** if there is no available seating to work at the second table.
 18. **Level and a selection of ca. 5-cm square pieces of plywood** of varying thicknesses to level the table for the light box.
 19. **Scissors, pruning shears, and small trowel** for collecting subjects.
 20. **Modeling clay** for supporting the subjects.
 21. **Alligator clips on wire and base** (two). The alligator clip (3 cm) is held at the end of a 13-cm piece of 12 awg copper wire with black insulation anchored in a heavy base

- a 3-cm drum knob). The pieces are glued together (e.g., with Gorilla glue) after the clip and the base are spray-painted matte black. Do not spray-paint the wire because it will flake off.
22. **Large galvanized bushing** spray-painted matte black to hold larger subjects on the turntable. We use a 4 cm × 3 cm (sold as 1.5 in × 1.25 in) bushing.
 23. **Bright LED flashlight** to brighten subject when using Live View to focus the lens.
 24. **Combination metric/imperial ruler** and **digital calipers** to measure the geometry of the subject.
 25. **Tape measure** to measure the heights of the cameras and distances from the subject.
 26. **Paintbrush** to remove debris from the subject.
 27. **Pencil** to create depressions in modeling clay for anchoring the subject and to record information during imaging.
 28. **Clipboard with paper** or **collecting notebook** to record activities.
 29. **Double-sided tape**
 30. **Cut-out of black fabric** the same size as the turntable (for use with black background). A pair of 10-cm scale bars were taped onto the black fabric.
 31. **1.5–2-mL Eppendorf (Hamburg, Germany) tubes filled with water**
 32. **Nalgene bottle filled with water**
 33. **Computer** (variable cost). Agisoft Metashape software (#37 below) has minimum requirements for the RAM, CPU, and GPU that can be found at <https://www.agisoft.com/downloads/system-requirements/>. Where practical, we encourage users to select computers that meet optimal, rather than minimum, specifications.
 - a. If a PC user, one might seek to model after the Alienware m15 R4 (Dell, Round Rock, Texas, USA) that we used, which had the following specifications: Intel(R) Core i9-10980HK CPU @ 2.40 GHz, 3096 Mhz, 8 Cores, 16 Logical Processors; 32.0 GB of RAM; NVIDIA GeForce RTX 3080 Laptop GPU <https://www.dell.com/ae/p/alienware-m15-r4-laptop/pd>
 - b. If a Mac user, one might seek to model after the MacBook Pro (Apple, Cupertino, California, USA) that we used, which had the following specifications: Apple M1 Max with 32 GB unified memory, 10-Core CPU, 16-Core GPU
34. **External SSD hard drive**. We use the same 4-TB external hard drive to store our images and our Metashape projects. We found the average storage space required for one of our modeling projects (including original RAW and JPG images, derivative images, associated project files, and a decimated PLY model) was about 45 GB when based on 192 images.
 - a. LaCie Rugged SSD Pro 4 TB with Thunderbolt 3 (1; \$999.99; LaCie, Paris, France) https://www.bhphotovideo.com/c/product/1636466-REG/lacie_sthz4000800_4tb_rugged_ssd_pro.html
 35. **Memory card reader**
 - a. Insignia USB 3.0 Memory Card Reader (1; Model NS-DCR30D3K, \$24.99; Insignia, Richfield, Minnesota, USA) <https://www.insigniaproducts.com/pdp/NS-DCR30D3K/5787403>
 36. **Agisoft Metashape Professional Edition software** (\$3499 listed, but ask about discount for educators, if applicable)
 - a. <https://www.agisoft.com/buy/online-store/>
 37. **ColorChecker Camera Calibration software** (free; X-Rite, Grand Rapids, Michigan, USA)
 - a. https://xritephoto.com/ph_product_overview.aspx?ID=1115&Action=Support&SoftwareID=2215
 38. **Adobe Lightroom** (Adobe, San Jose, California, USA), or comparable image editing software (free or variable cost, depending on organization's license agreement).
 - a. <https://www.adobe.com/products/photoshop-lightroom.html>
 39. **Microsoft Paint** (Microsoft, Redmond, Washington, USA), or comparable raster software such as **Adobe Photoshop** (free or variable cost, depending on organization's license agreement).
 - a. <https://apps.microsoft.com/store/detail/paint/9PCFS5B6T72H?hl=en-us&gl=us>